

# Apolipoprotein A-I Helsinki promotes intracellular acyl-CoA cholesterol acyltransferase (ACAT) protein accumulation

Juan D. Toledo · Horacio A. Garda · Laura V. Cabaleiro · Angela Cuellar ·  
Magali Pellon-Maison · Maria R. Gonzalez-Baro · Marina C. Gonzalez

Received: 19 October 2012 / Accepted: 30 January 2013 / Published online: 3 March 2013  
© Springer Science+Business Media New York 2013

**Abstract** Reverse cholesterol transport is a process of high antiatherogenic relevance in which apolipoprotein AI (apoA-I) plays an important role. The interaction of apoA-I with peripheral cells produces through mechanisms that are still poorly understood the mobilization of intracellular cholesterol depots toward plasma membrane. In macrophages, these mechanisms seem to be related to the modulation of the activity of acyl-CoA cholesterol acyltransferase (ACAT), the enzyme responsible for the intracellular cholesterol ester biosynthesis that is stored in lipid droplets. The activation of ACAT and the accumulation of lipid droplets play a key role in the transformation of macrophages into foam cells, leading to the formation of atheroma or atherosclerotic plaque. ApoA-I Helsinki (or  $\Delta$ K107) is a natural apoA-I variant with a lysine deletion in the central protein region, carriers of which have increased atherosclerosis risk. We herein show that treatment of cultured RAW macrophages or CHOK1 cells with  $\Delta$ K107, but not with wild-type apoA-I or a variant containing a similar deletion at the C-terminal region ( $\Delta$ K226), lead to a marked increase (more than 10 times) in the intracellular ACAT1 protein level as detected by western blot analysis. However, we could only detect a slight increase in

cholesteryl ester produced by  $\Delta$ K107 mainly when Chol loading was supplied by low-density lipoprotein (LDL). Although a similar choline-phospholipid efflux is evoked by these apoA-I variants, the change in phosphatidylcholine/sphingomyelin distribution produced by wild-type apoA-I is not observed with either  $\Delta$ K107 or  $\Delta$ K226.

**Keywords** Acyl-CoA cholesterol acyl transferase · Cholesterol efflux · Phospholipid efflux · Murine macrophages

## Introduction

Acyl-CoA cholesterol acyltransferase (ACAT) is the enzyme responsible for the intracellular cholesterol ester biosynthesis that is stored in lipid depots. Cholesterol mobilization and efflux compete with its esterification by ACAT and accumulation in lipid droplets, a key event in the transformation of macrophages in foam cells of atherosclerotic lesions. Apolipoprotein A-I (apoA-I) is the major protein of high density lipoproteins (HDL), and it plays a key role in reverse cholesterol transport, a process of high antiatherogenic relevance. Interaction of apoA-I with specific sites at the cell membrane triggers different signaling pathways, some of them resulting in mobilization of intracellular cholesterol toward cell membrane, making it available for the release toward HDL [1–6].

ApoA-I is mainly composed of type A amphipathic  $\alpha$ -helical repeats; two of them show a particular type Y charge distribution, one at the center and the other at the C-end, which have been proposed to play a key role in the apoA-I-mediated cell lipid efflux [7, 8]. Variants of apoA-I occur naturally. Some of them seem to exert a greater antiatherogenic effect than that of normal variants, as

---

Juan D. Toledo: member of Carrera del Profesional de Apoyo a la Investigación, CIC, Pcia. Bs. As. Argentina.

Horacio A. Garda, Magalí Pellón Maison, María R. González Baró and Marina C. Gonzalez: member of the Carrera del investigador Científico, CONICET, Argentina.

---

J. D. Toledo · H. A. Garda · L. V. Cabaleiro · A. Cuellar ·  
M. Pellon-Maison · M. R. Gonzalez-Baro · M. C. Gonzalez (✉)  
Facultad de Ciencias Médicas, Instituto de Investigaciones  
Bioquímicas de La Plata (INBIOLP), CONICET-UNLP,  
Universidad Nacional de La Plata, Calles 60 y 120,  
1900 La Plata, Argentina  
e-mail: marinacego@hotmail.com

R173C or apoAI-Milano [9]. Others have an increased risk of atherosclerosis for their carriers. Among them, there is a lysine deletion variant,  $\Delta$ K107 (Helsinki), present in 0.1 % of the population [10]. It was found to be related to low levels of HDL-cholesterol, deficiency of LpAI (lipoprotein with apoA-I but no apoA-II) and LpAI: AII (lipoprotein with both apoA-I and apoA-II) [11], hypertriglyceridemia, altered postprandial response, [3] and increased amyloidogenicity [12, 13], though the mechanisms triggering these symptoms are still poorly known.  $\Delta$ K107 is catabolized faster than the wild-type apoA-I [14, 15], and controversial results have been reported dealing with its capacity to activate LCAT [11, 12]. This mutant generates reconstituted discoidal HDL that cannot be remodeled by LDL [16]. Also, it has a lower capacity to bind to HDL and produce micellization of DMPC vesicles [17]. We have previously reported that in CHOK1 cells,  $\Delta$ K107 evokes a normal cholesterol efflux but it is unable to mobilize intracellular cholesterol depots as wild-type apoA-I does [18]. Deletion of K 107 would alter the helix registry of the central apoA-I domain, which was postulated to play a key role in the interaction of this protein and HDL complexes with membranes [8]. In the present work, we report a remarkable increase in ACAT level protein and different responses related to cellular lipid mobilization of RAW macrophages to  $\Delta$ K107, in comparison with wild-type apoA-I and a second mutant ( $\Delta$ K226) with a lysine deletion at the C-terminal region, which was also postulated to play a key role in the interaction of apoA-I with lipids [19].

## Materials and methods

### Cell culture

About  $5 \times 10^5$  RAW 264.7 cells were seeded on 6-well plates and incubated until confluence (1 day) with 2 ml of Dulbecco's Modified Eagle Medium (DMEM) supplemented with penicillin/streptomycin (100 units/ml) and 10 % FBS at 37 °C in a 5 % CO<sub>2</sub> atmosphere.

### Construction of recombinant wild-type apoA-I and variants of apoA-I ( $\Delta$ K107– $\Delta$ K226)

The cDNAs of wild-type apoA-I and  $\Delta$ K107 in the expression vector pET30 were kindly donated by A. Jonas, University of Illinois. They were modified by site-directed mutagenesis to introduce a Glu2Asp mutation to create a formic acid labil Asp-Pro peptide bond between residues 2 and 3, which permits specific chemical cleavage of the N-terminal His-Tag fusion peptide as described by Ryan et al. [20]. The Stratagene Quick Change kit was used and primers were: forward: 5'-GGCAGCAAGATGATCCCC

CCAGAGCCCC-3' and reverse: 5'-GGGGCTCTGGGGG GGATCATCTTGCTGCC-3'.

For the construction of  $\Delta$ K226, the modified cDNA for wild-type apoA-I was used as template and the primers were: forward: 5'-GCTGGAGAGCTTCGTCAGCTTCC TGAGC-3' and reverse: 5'-GCTCAGGAAGCTGAC GAA GCTCTCCAGC-3'.

The poly-His-tagged fusion proteins were purified by metal affinity chromatography and 45 % formic acid was used to cleave the His-tag.

### Purification of low-density lipoprotein (LDL)

LDL was isolated from human plasma in floating gradient by sequential ultracentrifugation in the presence of EDTA (1.019–1.063 g/ml) and by conventional chromatographic procedures. This preparation was dialyzed in Tris/HCl buffer pH 7.40 1 mM EDTA for 24 h. The resulting solution was adjusted to a protein concentration of 2–4 mg/ml, and bubbled under nitrogen or argon [21].

### MTT assay

To compare mitochondrial functioning in cholesterol-loaded and unloaded cells,  $2.5 \times 10^5$  RAW cells were incubated in 24 well plates for 24 h to confluence. Cells were incubated with increasing doses of Chol (20, 30, 40, 50, and 60  $\mu$ g/ml) in 10 % FBS DMEM for 24 h at 37 °C. The medium was removed and MTT (3-[4, 5-dimethylthiazol-2-yl]-2, 5-diphenyl tetrazolium bromide, 0.5 mg/ml) added and incubated 1 h at 37 °C. The MTT was removed and washed three times with PBS and then dimethyl sulfoxide was added to solubilize MTT formazan crystals. We have monitored the increase of optical density at 560 nm with background subtraction of 640 nm (unmetabolized MTT) using a Multimode Detector, DTX 880, Beckman-Coulter multiplate reader.

### Cholesterol efflux

To measure Chol efflux, RAW 264.7 cells were labeled with 50  $\mu$ g/ml Chol in 1 % fatty acid-free BSA-DMEM containing 0.05  $\mu$ Ci/ml <sup>14</sup>C cholesterol (Perkin Elmer) for 24 h. Control cells were incubated with Chol-free media. Alternatively, cells were loaded with LDL (50  $\mu$ g/ml Chol). Cells were then washed twice with PBS and allowed to equilibrate in culture medium containing 1 mg/ml BSA with 0.5 mM of 8-bromoadenosine-3-5-cyclic monophosphate (Br-cAMP) [22]. After 8-h equilibration, cells were washed and incubated for 12 h in DMEM at increasing doses of apoA-I (0, 10, 15, 20, 25 and 30  $\mu$ g/ml) maintaining the stimulus of Br-cAMP. In other efflux experiments, cells were treated in the presence or absence of 30  $\mu$ g/ml apoA-I and the

different mutant variants ( $\Delta K107$  and  $\Delta K226$ ). Background efflux was determined in control cells incubated with serum-free medium. Efflux media were collected and centrifuged to remove any detached cells and counted for  $^{14}C$ . Then, cells were scraped and solvent extracted for lipid analysis. Cellular lipids were extracted by the method of Bligh and Dyer [23]. Cholesterol efflux was calculated as the percentage of radioactivity in the medium relative to total radioactivity in cells plus medium.

#### Evaluation of cellular-free and esterified cholesterol and triacylglycerol content

Different Chol-loading conditions were used (0 and 50  $\mu g/ml$  Chol in culture medium and LDL added in a quantity equivalent to 50  $\mu g/ml$  Chol) to evaluate ACAT activity.

After the analysis of cholesterol removal with or without Br-cAMP, sterol species of cellular monolayers were analyzed by thin layer chromatography (TLC) on silica gel G plates developed in hexane: ethyl ether: acetic acid (80:20:1, v:v:v). Lipid spots corresponding to cholesteryl esters (CE) and non-esterified cholesterol were identified by staining with  $I_2$  vapor and co-migration with authentic standards. Then, the radioactivity in each lipid fraction was determined by Phosphor-Image using an ImageQuant TL (Storm) system. Also, we quantified the lipid mass using the reactive  $CuSO_4$  (10 %) in orthophosphoric acid [24, 25].

#### Efflux of choline-containing phospholipids

Cells were treated with medium containing BSA (2 mg/ml), unlabeled cholesterol (50  $\mu g/ml$ ), and  $^{14}C$ -phosphorylcholine (0.5  $\mu Ci/ml$ ) for 24 h. Cells were rinsed three times with PBS and equilibrated in appropriate culture medium (DMEM containing 0.5 mM Br-cAMP) for 8 h. Then, cells were treated with DMEM containing 30  $\mu g/ml$  of lipid-free apoA-I,  $\Delta K107$ , and  $\Delta K226$  for 18 h. Phospholipid efflux was calculated as the percentage of radioactivity in the medium relative to total radioactivity in cells plus medium.

#### Analysis of intracellular phosphatidylcholine and sphingomyelin

After the analysis of PL removal, polar lipid species of cell monolayers were separated by TLC on silica gel G plates developed in chloroform: methanol: acetic acid: water (50:37.5: 3.5: 2, v:v:v:v). Lipid spots corresponding to phosphatidylcholine (PC) and sphingomyelin (SM) were identified by staining with  $I_2$  vapor and co-migration with authentic standards. Then, the radioactivity in each lipid fraction was determined by Phosphor-Image using an ImageQuant TL (Storm) system.

#### ACAT1 protein level

Aliquots of the cellular monolayers were used for analyzing ACAT1 protein level. After separation of the cellular proteins by SDS-PAGE, immunoblotting was performed with a specific anti-ACAT1 primary antibody (Santa Cruz Biotechnology, Inc., dilution 1:200), HRP-conjugated secondary antibody (Thermo-Pierce, 1:1,000) and ECL detection.

#### Quantitative real-time PCR

RNA was extracted from samples using Trizol reagent (Invitrogen). Total RNA (1  $\mu g$ ) from samples was used for generating cDNA using the iScript cDNA synthesis kit (Bio-Rad). Equal amounts of cDNA (derived from 200 ng of total RNA) were amplified in triplicate with IQ Sybr Green Super Mix (Bio-Rad) using the Stratagene MX3000 apparatus. A no-template control and a no-reverse amplification control were included. Primers were designed to amplify the region between 44 and 226 of the open reading frame from mouse *Soat1* (forward primer: AGCAAGA TGAAGCCCAGAAA included in exon 2 and reverse ATGCGGACTTTTCAATGAGG included in exon 4). The thermal profile was 50 °C for 10 min, 95 °C for 5 min, and 40 cycles of 95 °C for 30 s, 60 °C for 1 min and 72 °C for 30 s. Fold changes in gene expression were determined using the  $\Delta Ct$  method with normalization to  $\beta$ -actin expression.

#### Other analytical methods

The mRNA levels were measured by quantitative real-time PCR using the Stratagene MX3000 apparatus.

Quantitative measurement of protein was performed by the method of Lowry et al. [26]. Student's *t* test was used for comparing pooled data.

## Results

#### Mitochondrial activity of RAW cells was not impaired by cholesterol loading

Considering that the experiments performed in this article implied cells Chol loading, we have tested the possible toxicity of Chol loading by employing MTT assay.

MTT assay, designed to evaluate mitochondrial metabolism and indirectly cell viability, showed no statistically significant differences between control cells and the ones loaded with cholesterol at our working doses and experimental time frame (24 h) (Fig. 1a, b). RAW cells have a metabolism adapted to store large amounts of neutral lipids

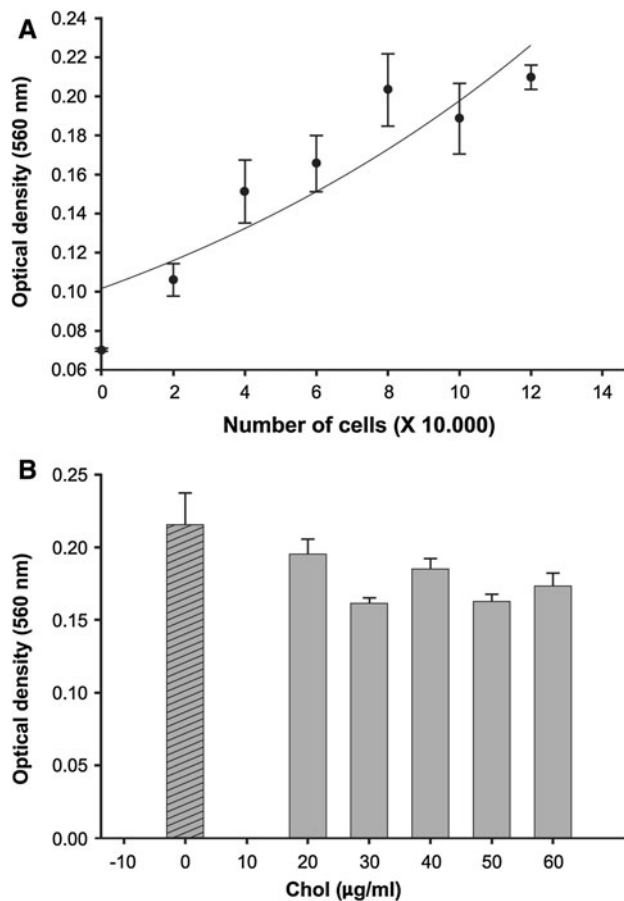


**Fig. 1** MTT assay: mitochondrial functioning in RAW 264.7 cells in function of **a** the cell concentration and **b** the treatment with different cholesterol concentrations (20–60 µg/ml) during 24 h. Bars represent the mean value of 3 independent experiments and the error bars represents SE

in comparison with other cell lines such as CHO, and they can resist high cholesterol doses (up to 60 µg/ml).

The three variants of apoA-I promote comparable cholesterol efflux in RAW cells

The efficiency to promote radiolabeled cholesterol removal from RAW cells was compared for  $\Delta$ K107,  $\Delta$ K226, and wild-type apoA-I. Results indicate that at 30 µg/ml apoA-I,  $\Delta$ K107, and  $\Delta$ K226 were as active as the wild-type form to remove cholesterol from RAW cells treated with Br-cAMP (Fig. 2), indicating that both mutated forms of apoA-I were functional.

Evaluation of cellular-free and esterified cholesterol and triacylglycerol (TG) mass

To evaluate the effect of Chol loading and the different supply of Chol to cells (Chol-free or Chol-LDL) on cellular

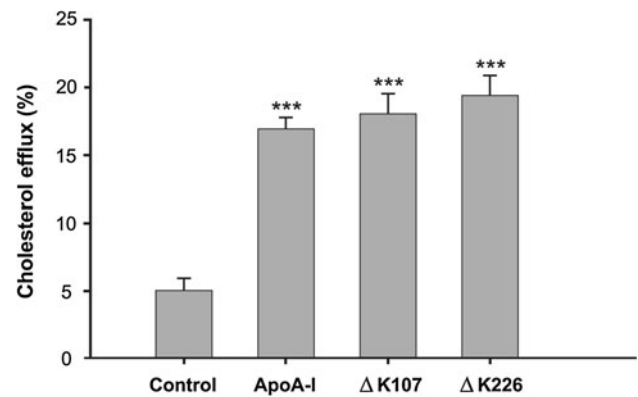


**Fig. 2** Analysis of cholesterol removal from RAW cells by apoA-I variants. Significance was calculated with student's *t* test with respect to control ( $***P \leq 0.001$ ). Bars represents the mean value of 3 independent experiments and the error bars represents SE

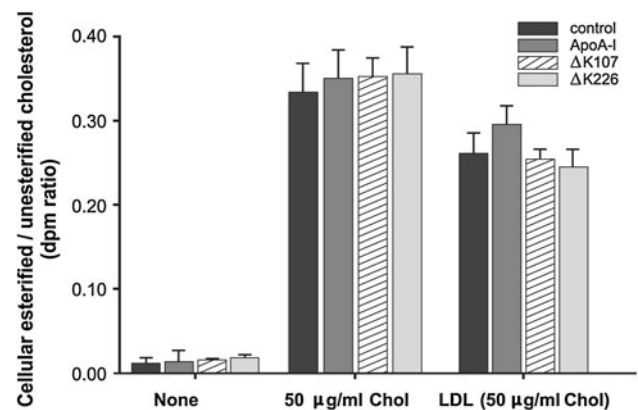


**Fig. 3** Analysis of cellular-free and esterified cholesterol radioactivity in RAW cells treated with Br-cAMP, under different cholesterol-loading conditions. Bars represent the mean value of 3 independent experiments and the error bars represents SE

Chol esterification mediated by ACAT, we have measured cholesteryl ester/cholesterol (CE/Chol) ratio.

In RAW cells, cholesterol loading remarkably enhances CE/Chol radioactivity ratio (Fig. 3). The treatment with LDL (50 µg/ml Chol) produced a lower increment of this ratio than the treatment with 50 µg/ml of albumin-vehicle-lyzed cholesterol (Fig. 3).

The increment of CE/Chol values in Chol-loaded macrophages with respect to unloaded cells was more than tenfold in cells treated with Br-cAMP and sixfold in untreated cells. The higher values of CE/Chol radioactivity ratio in Br-cAMP-untreated RAW cells evidence a larger amount of Chol available to be esterified. We could not evidence any change in CE/Chol radioactivity by apoA-I and their variants with respect to control (Fig. 3) in macrophages treated with Br-cAMP. However, in RAW cells without Br-cAMP treatment and loaded with free Chol or

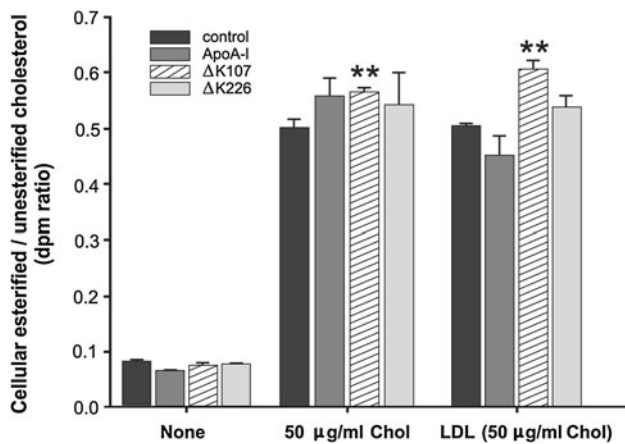


**Fig. 4** Analysis of cellular-free and esterified cholesterol radioactivity in RAW cells treated without Br-cAMP, under different cholesterol-loading conditions. Bars represent the mean value of 3 independent experiments and the error bars represents SE

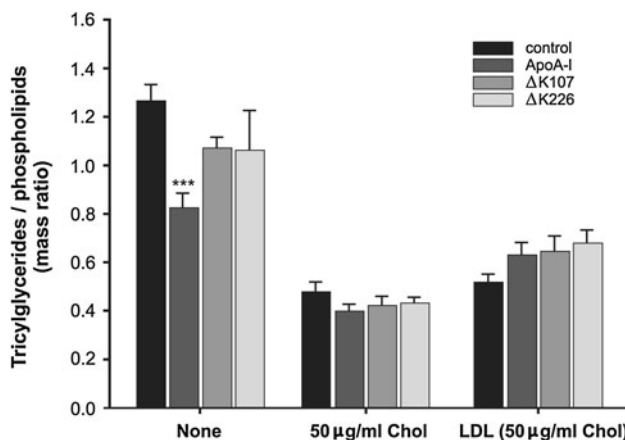


**Fig. 5** Analysis of cellular TG/FL mass in RAW cells treated with Br-cAMP, under different cholesterol-loading conditions ( $***P \leq 0.001$ ). Bars represent the mean value of 3 independent experiments and the error bars represents SE

LDL, we have observed that CE/Chol radioactivity ratio enhances only after treatment with  $\Delta K107$  (Fig. 4).

As shown in Fig. 5, cholesterol loading of macrophages results in a decreased TG/PL mass ratio. We have also observed that only the treatment with apoA-I diminishes TG/PL mass ratio in cells that have not been Chol-loaded. However, in cells loaded with free Chol or LDL, TG/PL mass ratio is not affected by the treatment with apoA-I or its variants (Fig. 5).

Choline-containing phospholipid efflux and analysis of phospholipids remaining in cell monolayers

To determine the efficiency of promoting phospholipid efflux of apoA-I and its mutant forms, we labeled Chol-loaded RAW cells with  $^{14}C$ - phosphorylcholine, incubated

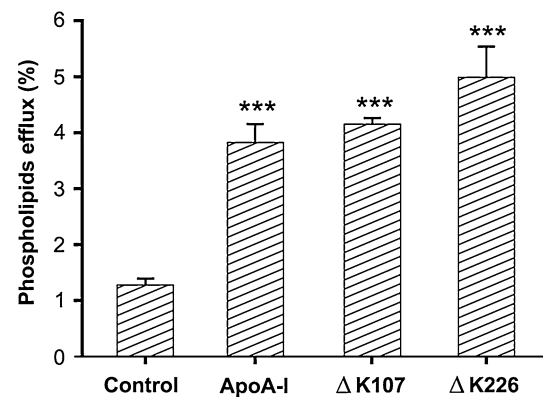


**Fig. 6** Analysis of choline-phospholipid removal by apoA-I variants ( $***P \leq 0.01$ ). Bars represent the mean value of 3 independent experiments and the error bars represents SE

**Table 1** Influence of apoA-I variants on the distribution of radioactive choline between SM and PC fractions ( $***P \leq 0.01$ ,  $*P \leq 0.05$ )

$^{14}C$ -PC/SM ratio			
Control	ApoA-1	$\Delta K107$	$\Delta K226$
$6.14 \pm 0.47$	$3.61 \pm 0.65^*$	$6.18 \pm 0.29$	$6.02 \pm 0.66$

Bars represent the mean value of 3 independent experiments and the error bars represents SE

them with or without 30  $\mu g/ml$  apoA-I and quantified the radioactivity in the culture medium. Efflux of choline-phospholipids after 18-h incubation was similar for apoA-I,  $\Delta K107$ , and  $\Delta K226$  but significantly higher than for no-protein controls (Fig. 6). By analyzing the lipid extract of RAW cell monolayers, we detected radioactivity mostly in PC and scarcely in SM. After 18-h incubation, PC/SM ratio significantly diminished compared to control when cells were treated with apoA-I, but not with the mutants  $\Delta K107$  or  $\Delta K226$  (Table 1). Consistently, previous results with apoA-I and different types of rHDL [27] showed that after 18-h treatment PC/SM radioactivity ratio significantly decreased. We now show that deletion of the lysine residue in position 107 or K226 results in the loss of this capacity.

$\Delta K107$  treatment results in cellular accumulation of ACAT1 protein

As we have mentioned above the enzyme ACAT is very important in the formation of CE depots in atherosclerotic lesions. Considering the proatherogenic apoA-I Helsinki profile, we have evaluated the effect of this natural mutant apoA-I on ACAT enzyme level.

The influence of apoA-I and both lysine deletion mutants on the cellular level of ACAT1 protein was measured by immunoblotting. In RAW cells under different cholesterol-loading conditions (0, 10 and 50  $\mu g/ml$  of



**Fig. 7** Effect of the treatment with apoA-I variants on the expression level of ACAT1. **a** RAW cells were loaded with free Chol or LDL-Chol (50  $\mu$ g/ml) and further stimulated with apoA-I,  $\Delta$ K107 and  $\Delta$ K226; **b** RAW cells were loaded with 0 or 10  $\mu$ g/ml and further stimulated with apoA-I,  $\Delta$ K107, and  $\Delta$ K226; **c** CHOK1 cells loaded with 50  $\mu$ g/ml Chol were treated with apoA-I variants, only the treatment with  $\Delta$ K107 produce increment expression of ACAT1. Bars represent the mean value of 3 independent experiments and the error bars represents SE

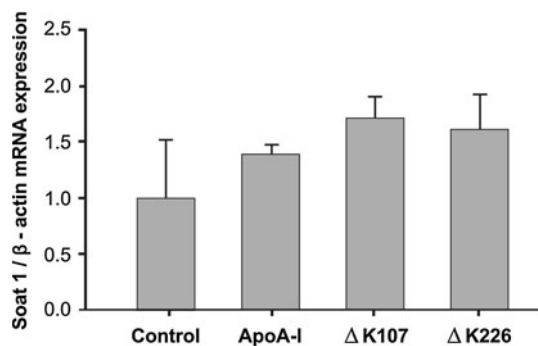
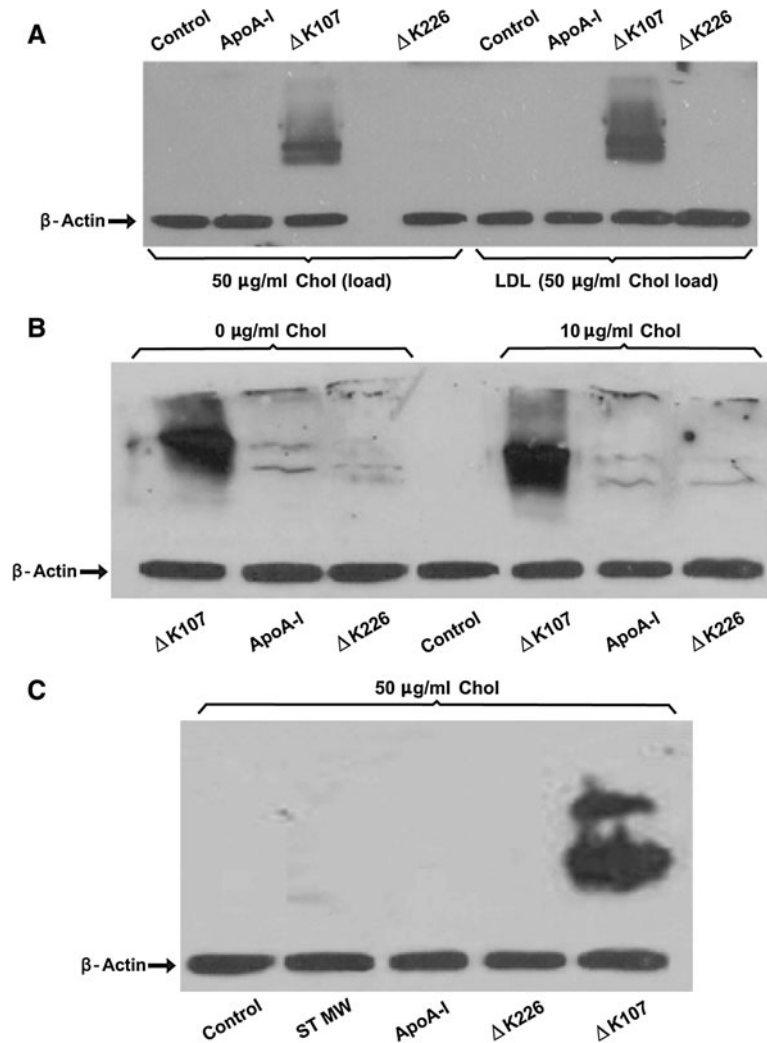


**Fig. 8** SOAT 1 (or ACAT1) mRNA expression. RAW cells were loaded with free Chol (50  $\mu$ g/ml) and further stimulated with apoA-I,  $\Delta$ K107, and  $\Delta$ K226. Bars represent the mean value of 3 independent experiments and the error bars represents SE

albumin-vehiculized cholesterol and 50  $\mu$ g/ml of LDL-vehiculized cholesterol), a remarkable increase of the cellular ACAT1 protein level was produced by the treatment with the mutant  $\Delta$ K107, but not with  $\Delta$ K226 or wild-type apoA-I during 12 h. (Fig. 7a, b). Also in CHOK1 and

THP1 cells (not shown) loaded with 50  $\mu$ g/ml Chol, only the treatment with  $\Delta$ K107 increments ACAT1 protein level (Fig. 7c) indicating that this fact is not exclusive for murine macrophages.

We have also evaluated the ACAT1 mRNA level by the real-time PCR technique. We were not able to see any significant change in the amount of ACAT1 mRNA when the cells were treated with apoA-I and their lysine deletion variants with respect to control (Fig. 8).

## Discussion

Macrophages play key roles in atherosclerosis. Cholesterol loading transforms them in foam cells, which can accumulate in the arterial wall but may also respond to specific acceptors for cholesterol transport to liver. A key event for the transformation of macrophages in foam cells is the activation of ACAT1 leading to an increased uptake of modified LDL, accumulation of cholesteryl esters, and

decreased cholesterol efflux to HDL [28]. It is shown in this work that the treatment of murine macrophages with  $\Delta$ K107 produces an increment of more than ten folds in the ACAT1 cellular level detected by western-blotting with a specific antibody. This effect is specific for the variant with the lysine deletion at the central region, since it is not produced by the lysine deletion at the C-terminus ( $\Delta$ K226) or the wild-type apoA-I; and this effect could have pathophysiological relevance and be related to the increased atherogenic risk observed in patients carrying the  $\Delta$ K107 mutation. The importance of apoA-I Helsinki ( $\Delta$ K107) mutation is because patients have decreased serum HDL Chol, LpA-I, and LpA-I:A-II levels, reduced cholesteryl ester transfer protein activity (CETP) which may be associated with premature coronary heart disease.

ACAT1 protein accumulation evoked by  $\Delta$ K107 in RAW cells is independent of cholesterol-loading conditions. In spite of the increase in ACAT1 protein level produced by the treatment of RAW cells with  $\Delta$ K107 and Br-cAMP, we could not prove an increase in CE/Chol radioactivity ratio. Moreover, we have quantified Chol and CE mass in Raw cells loaded with free Chol or LDL. We measured an increment in CE/Chol mass ratio produced by  $\Delta$ K107 only in macrophages pre-loaded with LDL (not shown) RAW Chol loading and further stimulation with cAMP analog (Br-cAMP) stimulate ABCA1 transporter and Chol efflux. Therefore, cholesterol mobilization and efflux compete with its esterification by ACAT and accumulation in lipid droplets. Another possibility that could explain our results is a possible concurrent overexpression of cholesteryl ester hydrolases when the cells are treated with Br-cAMP. Related to this, Brown and Col [29] demonstrated that stored cytoplasmic cholesteryl esters in macrophages are constantly undergoing a cycle of hydrolysis and re-esterification.

However, in macrophages not treated with Br-cAMP, we were able to see an increase in CE/Chol radioactivity ratio only in cells stimulated with  $\Delta$ K107 with respect to control. This effect was produced only in cells loaded with either free cholesterol or LDL. This result could be explained because cholesterol efflux is higher in Br-cAMP treated-RAW cells than in the untreated ones. Thus, cholesterol availability for esterification is increased and we could see the differential effect produced by  $\Delta$ K107. It is important to note that the increment in ACAT1 level is not comparable in magnitude to the increase in CE/Chol radioactivity ratio.

The increment of ACAT1 produced by  $\Delta$ K107 does not seem to be specific for macrophages, since it has been also observed in CHOK1 cells. We have previously described [18] that treatment of CHOK1 cells with  $\Delta$ K107 results in a higher CE/Chol radioactivity ratio compared with the treatment with wild-type apoA-I. This fact, however,

cannot be totally attributed to the increased cellular level of ACAT1 protein in  $\Delta$ K107-treated cells, since its CE/Chol radioactivity ratio is similar to that found in non-apolipoprotein-treated control cells which have a normal level of ACAT1 protein. We must highlight that RAW and CHOK1 cells behave differently considering intracellular CE accumulation and the response to apoA-I [27]. As herein shown, RAW cells can accumulate large amounts of CE in response to external cholesterol loading without any observable impairment in cell viability or mitochondrial functioning.

Among the possibilities that could explain the difference between the magnitude in the increment in ACAT1 level and the increase in CE/Chol radioactivity ratio, we can mention: (a) the accumulation of an inactive form of ACAT1 or (b) its accumulation at an unfavorable cellular compartment with reduced accessibility to the exogenously added cholesterol.

We have also shown here that ACAT1 protein accumulation is not accompanied by an enhanced mRNA level, suggesting that it is due to an increased translation rate or to a decreased protein degradation rate. Regarding this fact, it was reported that the HDL-2 fraction inhibits ACAT activity in murine macrophage cultures, but it increases their synthesis and turnover rates without modifying the total amount of the enzyme [30]. Moreover, HDL-2 promotes ACAT translocation from perinuclear compartments of the endoplasmic reticulum toward vesicular structures in the cellular periphery near plasma membrane. Experimental data support that ACAT inhibition by HDL-2 would be the consequence of the translocation to an inactive cellular compartment, and authors propose that HDL-2 behaves as an initiating factor in a signal transduction pathway leading to intracellular ACAT translocation and inactivation. It is very likely that the reported action of HDL-2 is due to its major apolipoprotein, apoA-I. If so, the deletion of lysine at position 107 could result in an altered signaling pathway/s leading to the ACAT1 protein accumulation observed in this work. Other studies [31, 32] are also indicative that distribution of ACAT1 between active and inactive compartments plays a role in the enzyme activation in response to cholesterol loading and macrophage transformation into foam cells.

Another observation made in this work concerns the differential effects of wild-type apoA-I and lysine deletion mutants on the cellular triacylglycerol and cholinephospholipid distribution. Although all the apoA-I variants were similarly active in promoting PC efflux, only wild-type apoA-I was able to decrease the cellular PC/SM ratio. Also, only the wild-type variant decreases the TG/PL mass ratio in cells not loaded with cholesterol. These actions of apoA-I are lost in both tested mutants ( $\Delta$ K107 and  $\Delta$ K226) indicating that both lysine residues are essentials. The effect

of apoA-I on the cellular TG/PL ratio is not observed in cholesterol-loaded macrophages. Probably, TG/PL mass ratio decreases to replenish PL removal from cellular TG generated by specific intracellular lipid traffic, which would be promoted mainly by apoA-I. At high cholesterol loading, both Chol efflux and Chol esterification are stimulated, this latter could be done with fatty acids originated by TG hydrolysis, but at the same time also PL efflux are promoted by apoA-I. Therefore, TG/PL mass ratio is barely modified. In cells loaded with LDL, the lipoprotein also supplies fatty acids and extra lipids besides Chol, which could explain a tendency to increase TG/PL mass ratio, considering that apoA-I and both mutants are active to promote Chol and PL efflux.

In summary, we have demonstrated that though lysine deletion at position 107 or 226 does not affect the ability of apoA-I to stimulate Chol and PL efflux, both deletions affect the ability of apoA-I to redistribute cellular TG and choline-phospholipids. The lysine deletion at 107 position (apoA-I Helsinki) produces a remarkable accumulation of ACAT-1 protein which is related to an increment in CE/Chol only in macrophages non-treated with Br-cAMP. More studies will be necessary to understand the relationship of these results with the increased atherogenic risk of  $\Delta$ K107 holder patients.

**Acknowledgments** This work was supported by Grants: PICT 26228 and 2106 from ANPCyT, Argentina and PIP 00953 from CONICET. National Institutes of Health TW06034 (MRGB), ANPCyT PICT 2246 (MRGB). MCG and HAG are members of Carrera del Investigador científico from CONICET. The authors thank Laura Hernandez and Mario Gómez for their technical assistance.

## References

- Sviridov D, Fidge N, Beaumier-Gallon G, Fielding C (2001) Apolipoprotein A-I stimulates the transport of intracellular cholesterol to cell-surface cholesterol-rich domains (caveolae). *Biochem J* 358:79–86
- Yamauchi Y, Chang CC, Hayashi M, Abe-Dohmae S, Reid PC et al (2004) Intracellular cholesterol mobilization involved in the ABCA1/apolipoprotein-mediated assembly of high density lipoprotein in fibroblasts. *J Lipid Res* 45:1943–1951
- Li Q, Yokoyama S (1995) Independent regulation of cholesterol incorporation into free apolipoprotein-mediated cellular lipid efflux in rat vascular smooth muscle cells. *J Biol Chem* 270:26216–26223
- Li Q, Tsujita M, Yokoyama S (1997) Selective down-regulation by protein kinase C inhibitors of apolipoprotein-mediated cellular cholesterol efflux in macrophages. *Biochemistry* 36:12045–12052
- Ito J, Nagayasu Y, Ueno S, Yokoyama S (2002) Apolipoprotein-mediated cellular lipid release requires replenishment of sphingomyelin in a phosphatidylcholine-specific phospholipase C-dependent manner. *J Biol Chem* 277:44709–44714
- Nofer JR, Feuerborn R, Levkau B, Sokoll A, Seedorf U et al (2003) Involvement of Cdc42 signaling in apoA-I-induced cholesterol efflux. *J Biol Chem* 278:53055–53062
- Corsico B, Toledo JD, Garda HA (2001) Evidence for a central apolipoprotein A-I domain loosely bound to lipids in discoidal lipoproteins that is capable of penetrating the bilayer of phospholipid vesicles. *J Biol Chem* 276:16978–16985
- Toledo JD, Prieto ED, Gonzalez MC, Soulages JL, Garda HA (2004) Functional independence of a peptide with the sequence of human apolipoprotein A-I central region. *Arch Biochem Biophys* 428:188–197
- Franceschini G, Calabresi L, Chiesa G, Parolini C, Sirtori CR et al (1999) Increased cholesterol efflux potential of sera from ApoA-IMilano carriers and transgenic mice. *Arterioscler Thromb Vasc Biol* 19:1257–1262
- Rall SC Jr, Weisgraber KH, Mahley RW, Ogawa Y, Fielding CJ et al (1984) Abnormal lecithin:cholesterol acyltransferase activation by a human apolipoprotein A-I variant in which a single lysine residue is deleted. *J Biol Chem* 259:10063–10070
- Tilly-Kiesi M, Zhang Q, Ehnholm S, Kahri J, Lahdenpera S et al (1995) ApoA-I Helsinki (Lys107→0) associated with reduced HDL cholesterol and LpA-I:A-II deficiency. *Arterioscler Thromb Vasc Biol* 15:1294–1306
- Tilly-Kiesi M, Lichtenstein AH, Rintaraho J, Taskinen MR (1998) Postprandial responses of plasma lipids and lipoproteins in subjects with apoA-I(Lys107→0). *Atherosclerosis* 137:37–47
- Amarzguioui M, Mucchiano G, Haggqvist B, Westermark P, Kavlie A et al (1998) Extensive intimal apolipoprotein AI-derived amyloid deposits in a patient with an apolipoprotein AI mutation. *Biochem Biophys Res Commun* 242:534–539
- Mucchiano GI, Haggqvist B, Sletten K, Westermark P (2001) Apolipoprotein A-I-derived amyloid in atherosclerotic plaques of the human aorta. *J Pathol* 193:270–275
- Tilly-Kiesi M, Lichtenstein AH, Ordovas JM, Dolnikowski G, Malmstrom R et al (1997) Subjects with ApoA-I(Lys107→0) exhibit enhanced fractional catabolic rate of ApoA-I in Lp(AI) and ApoA-II in Lp(AI with AII). *Arterioscler Thromb Vasc Biol* 17:873–880
- Lee JH, Reed DR, Li WD, Xu W, Joo EJ et al (1999) Genome scan for human obesity and linkage to markers in 20q13. *Am J Hum Genet* 64:196–209
- Jonas A, von Eckardstein A, Churgay L, Mantulin WW, Assmann G (1993) Structural and functional properties of natural and chemical variants of apolipoprotein A-I. *Biochim Biophys Acta* 1166:202–210
- Gonzalez MC, Toledo JD, Tricerri MA, Garda HA (2008) The central type Y amphipathic  $\alpha$ -helices of apolipoprotein AI are involved in the mobilization of intracellular cholesterol depots. *Arch Biochem Biophys* 473:34–41
- Oda MN, Forte TM, Ryan RO, Voss JC (2003) The C-terminal domain of apolipoprotein A-I contains a lipid-sensitive conformational trigger. *Nat Struct Biol* 10:455–460
- Ryan RO, Forte TM, Oda MN (2003) Optimized bacterial expression of human apolipoprotein A-I. *Protein Expr Purif* 27:98–103
- Claise C, Edeas M, Chaouchi N, Chalas J, Capel L et al (1999) Oxidized-LDL induce apoptosis in HUVEC but not in the endothelial cell line EA.hy 926. *Atherosclerosis* 147:95–104
- Smith JD, Miyata M, Ginsberg M, Grigaux C, Shmookler E et al (1996) Cyclic AMP induces apolipoprotein E binding activity and promotes cholesterol efflux from a macrophage cell line to apolipoprotein acceptors. *J Biol Chem* 271:30647–30655
- Bligh EG, Dyer WJ (1959) A rapid method of total lipid extraction and purification. *Can J Biochem Physiol* 37:911–917
- Gennaro LA, Fried B, Sherma J (1996) HPTLC determination of phospholipids in snail conditioned water from *Helisoma trivolvis* and *Biomphalaria glabrata*. *J Planar Chromatogr* 9:379–381



25. Frazer B, Reddy A, Fried B, Sherma J (1997) Effects of diet on the lipid composition of *Echinostoma caproni* (Trematoda) in ICR mice. *Parasitol Res* 83:642–645
26. Lowry OH, Rosebrough NJ, Farr AL, Randall RJ (1951) Protein measurement with the Folin phenol reagent. *J Biol Chem* 193:265–275
27. Toledo JD, Cabaleiro LV, Garda HA, Gonzalez MC (2012) Effect of reconstituted discoidal high-density lipoproteins on lipid mobilization in RAW 264.7 and CHOK1 cells. *J Cell Biochem* 113:1208–1216
28. Meuwese MC, de Groot E, Duivenvoorden R, Trip MD, Ose L et al (2009) ACAT inhibition and progression of carotid atherosclerosis in patients with familial hypercholesterolemia: the CAPTIVATE randomized trial. *JAMA* 301:1131–1139
29. Brown MS, Ho YK, Goldstein JL (1980) The cholesteryl ester cycle in macrophage foam cells. *J Biol Chem* 255:9344–9352
30. Li L, Pownall HJ (2000) Regulation of acyl-coenzyme A: cholesterol acyltransferase (ACAT) synthesis, degradation, and translocation by high-density lipoprotein(2) at a low concentration. *Arterioscler Thromb Vasc Biol* 20:2636–2642
31. Sakashita N, Miyazaki A, Takeya M, Horiuchi S, Chang CC et al (2000) Localization of human acyl-coenzyme A: cholesterol acyltransferase-1 (ACAT-1) in macrophages and in various tissues. *Am J Pathol* 156:227–236
32. Sakashita N, Chang CC, Lei X, Fujiwara Y, Takeya M et al (2010) Cholesterol loading in macrophages stimulates formation of ER-derived vesicles with elevated ACAT1 activity. *J Lipid Res* 51:1263–1272